Open Access, April 2024
p-ISSN : 2087-9423
e-ISSN : 2620-309X

Jurnal Ilmu dan Teknologi Kelautan Tropis, 16(1): 1-26
DOI: https://doi.org/10.29244/jitkt.v16i1.48399
Available online at https://journal.ipb.ac.id/index.php/jurnalikt

THE IMPACT SHORELINE MODIFICATIONS ON LEKANG TURTLE (*Lepidochelys olivacea*) CONSERVATION ALONG COASTAL OF KULONPROGRO, INDONESIA

Waluyo*, Annisa Novita Sari, Khalila Fira Rufaida
Department of Aquaculture, Faculty of Agriculture, Tidar University, Magelang, Indonesia
*Corresponding author: waluyo@untidar.ac.id
(Received 21-07-2023; Revised 01-12-2023; Accepted 11-03-2024)

ABSTRACT

Changes in oceanographic circumstances that continue to occur will generate challenges for coastal ecology, one of which is a change in the sea-land boundary. It is possible to have an impact on the olive ridley turtles that rise to lay their eggs by changing the region of this coastal area, particularly at Trisik Beach, Kulonprogo, and Yogyakarta Special Region. The goal of this study was to use a Geographic Information System to estimate the effect of changes in the coastline on the distribution of olive ridley turtles on Trisik Beach, Kulon Progo, and Yogyakarta Special Region in 2020-2022. Digitizing the shoreline reveals changes in the coastline, which is then analyzed using Landsat 8 satellite data retrieved with ArcGIS software. The Landsat 8 photos span the years 2020-2022. Using the Digital Shoreline Analysis System (DSAS) toolbox, each image will go through area cropping or image cutting, geometric and radiometric correction, demarcation or development of a land-sea boundary line, on-screen digitalization, and automatic calculation of coastal changes. Trisik Beach's coastline alterations from 2020 to 2022 tended to create abrasion due to the shrinking beach area. The greatest average distance to a coastline alteration was -29.61 m, the smallest was -15.03 m, and the average speed of the greatest abrasion is -8.26 m/year, the smallest is -4.19 m/year, resulting in a 111,967.03 m^2 reduction in coastal area. The association between shoreline alterations and the distribution of olive ridley turtle nesting on Trisik Beach is quite significant, with the beach area affecting 91.3% of turtle nests and 88.5% of turtle eggs.
Keywords: Abrasion, conservation, distribution, shoreline, turtle

Dampak Perubahan Garis Pantai terhadap Konservasi Penyu Lekang (*Lepidochelys Olivacea*) di Sepanjang Pantai Kulonprogo, Indonesia

ABSTRAK

Perubahan kondisi oseanografi yang terus terjadi akan mengakibatkan masalah terhadap ekologi wilayah pesisir, salah satunya adalah pergeseran batas antara laut dan daratan. Dengan berubahnya luasan wilayah pesisir ini, khususnya di Pantai Trisik, Kulonprogo, Daerah Istimewa Yogyakarta, dimungkinkan dapat memberikan pengaruh terhadap penyu lekang yang naik untuk bertelur. Tujuan penelitian ini adalah untuk mengetahui pengaruh perubahan garis pantai terhadap distribusi penyu lekang di Pantai Trisik, Kulon Progo, Daerah Istimewa Yogyakarta pada tahun 2020-2022 dengan pendekatan Sistem Informasi Geografis. Perubahan garis pantai diketahui dengan cara digitasi garis pantai, dan garis pantai diolah melalui citra satelit Landsat 8 yang telah diperoleh dengan software ArcGIS. Citra Landsat 8 yang diambil meliputi tahun 2020-2022. Masing-masing citra akan dilakukan cropping area atau pemotongan citra, koreksi geometrik dan radiometrik, delininiasi atau pembuatan garis batas antara daratan dan laut, digitasi on screen, dan perhitungan perubahan garis pantai secara otomatis menggunakan toolbox Digital Shoreline Analysis System (DSAS). Perubahan garis pantai yang terjadi di Pantai Trisik selama tahun 2020-2022 cenderung mengalami abrasi karena luasan pantai yang semakin berkurang, nilai jarak rata-rata perubahan garis pantai tertinggi -29,61 m terendah -15,03 m, dan nilai rata-rata laju abrasi tertinggi -8,26 m/tahun, terendah –4,19 m/tahun yang mengakibatkan pengurangan luasan wilayah pantai sebesar 111.967,03 m^2. Korelasi antara perubahan garis pantai dengan distribusi peneluran penyu lekang di Pantai Trisik memiliki hubungan yang sangat kuat, luas pantai memengaruhi 91,3% jumlah sarang dan 88,5% jumlah telur penyu.
Kata kunci: *Abrasi, distribusi, garis pantai, penyu, konservasi*

INTRODUCTION

Indonesia has a relatively large water area, which is dominated by seawater. Indonesia has a 95,181 km long coastline with a sea area of 5.8 million km^2 (Wisudo, 2012) This means that Indonesia's sea waters contain significant and potentially valuable marine water resources, such as marine biological and non-biological variety (MMAF, 2010), one of which is turtles. A turtle is a reptile that spends the majority of its life in the sea. Green turtles (*Chelonia mydas*), olive ridley turtles (*Lepidochelys olivacea*), loggerhead turtles (*Caretta caretta*), hawksbill turtles (*Eretmochelys imbricata*), leatherback turtles (*Dermochely coriacea*), kempi's ridley turtles (*Lepidochelys kempi*), and flatback turtles (*Natator depressus*).

The seven turtles are fully protected because the International Union for Conservation of Nature (IUCN) has classified them as endangered or on the "red list," and they have Appendix 1 status in the Convention on International Trade in Endangered Species of Wild Fauna and Flora (CITES), which means that all types of international trade are prohibited. The decreasing turtle population was caused by a variety of hazards, including the taking of turtle eggs for commerce, the capturing of mother turtles, and turtle deaths as a result of becoming entangled in fishing activities (MMAF, 2015). Other risks, however, are uncontrollable, such as natural forces such as changes in oceanographic conditions and climate change, which endanger the turtles' habitat. Changes in coastal oceanographic circumstances can have an impact on existing coastal biological changes, one of which is a shift in coastal geomorphology.

The beach, which is part of this coastal area, is vulnerable to a variety of issues that endanger the sustainability of coastal and marine resources, such as pollution, physical degradation of habitats, overexploitation of natural resources, coastal abrasion, conservation of protected areas for other development purposes, and natural disasters (Waluya, 2008). Based on the existing shoreline, coastal geomorphological changes caused by these issues can be detected. The coastline is the boundary between the land area and the sea area, which are constantly changing and interacting with each other, experiencing temporary changes such as tides as well as long-term changes due to abrasion and accretion, so that the area produces a unique ecological environment and is vulnerable to change (Ismail, 2017).

Land reduction (abrasion) or land addition (acreage) can cause changes in the coastline (Setiani, 2017). Yogyakarta Province has experienced abrasion and accretion in three regencies in the 2004-2014 range, namely in Kulonprogo Regency, where there was abrasion of 7,528 ha of accretion of 24,464 ha, Bantul Regency had abrasion of 21,042 ha of accretion of 33,800 ha, and Gunungkidul Regency had abrasion of 67,967 ha of accretion of 41,900 ha (Hartri *et al*., 2015). Meanwhile, between 1999 and 2016, the coastline area of Kulonprogo Regency saw the worst abrasion in the Trisik Beach area, which was 219.5 meters caused by big waves and Progo River Estuary overflows (Cahyono *et al*., 2017). The shoreline change might cause the amount of the coastal area to shrink or increase, changes in turtle nesting may occur.

Trisik Beach, Kulonprogo, and the Special Region of Yogyakarta are among the turtle landing spots in Indonesia especialy *Lepidochelys olivacea*. There is also the Eternal Turtle Conservation Group in this area, which is run by environmental activists and has been protecting sea turtle eggs since 2004. This conservation action is carried out in the context of protecting sea turtles from predators and human poaching by conserving sea turtle eggs along the coast. However, because the coastline at Trisik Beach has undergone relatively dynamic

changes, it is vital to investigate the implications of these changes on the distribution of turtle nests. This was done to determine the association between the distribution of olive ridley turtle eggs (*Lepidochelys olivacea*) on Trisik Beach and coastal modifications. It is believed that this research would help the management of Eternal Turtle Conservation carry out conservation activities for the Lekang Turtle (*Lepidochelys olivacea*) in the future, allowing their population to be saved. The goal of this research was to see how changes in the shoreline affected the distribution of olive ridley turtle eggs on Trisik Beach, Kulonprogo, and the Special Region of Yogyakarta in 2020-2022.

RESEARCH METHODS

Time and Location of Research

This research was carried out in Trisik Beach, Kulonprogo Regency, Special Region of Yogyakarta, Central Java, in December 2022. Site surveys and direct data collection were carried out at Trisik Beach, Kulonprogo Regency, Special Region of Yogyakarta, before sand samples were analyzed at the Laboratory of the Faculty of Agriculture, Tidar University. Map of the research location is shown in Figure 1.

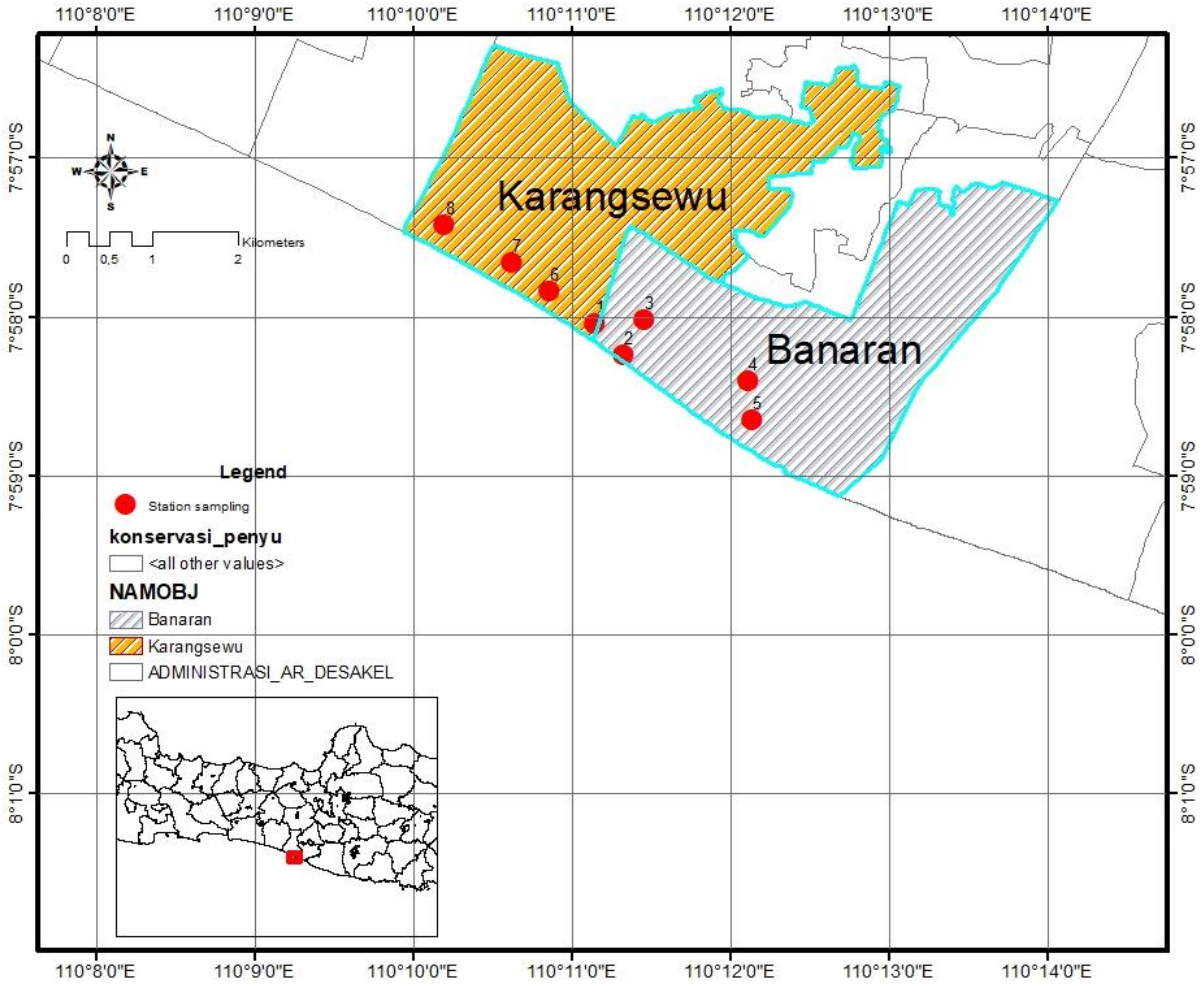

Figure 1. Research Location in Trisik Beach, Kulonprogo Regency, Special Region of Yogyakarta, Central Java.

Tools and Materials

The tools used in this research include the Global Positioning System (GPS), Envi 5.3 software, ArcGIS 10.4 software, Ocean Data View (ODV) software, roll meters, geological compasses, ovens, sieve shakers, and digital scales. The tools used to support this research activity are presented in Table 1. The materials used in this research include Landsat 8 imagery data for 2020–2022, data on olive ridley turtle nests and eggs at the Perennial Turtle Conservation, wind data, wave data, current data, and tide data, as well as beach sand samples taken at Trisik Beach. The research materials are listed in Table 2.

Collecting Data

Primary data is information gathered directly in the field through ground checks or field surveys. The survey was carried out at research stations chosen from areas where olive ridley turtle nests are frequently seen. Field surveys were done to collect data on beach slope, beach width, sediment sample, and verification of the research area's presence for use as supporting data.

Beach Length

The width of the beach to be measured is the supratidal width of the beach, using a roll meter. The supratidal width is calculated by measuring the distance between the outside vegetation and the highest tide on the coast.

Slope on The Beach

The coast's slope will be measured with a gadget resembling a geological compass. The slope measurement with a geological

Table 1. The tools used in this research

No.	Tools	Function
1.	Global Positioning System (GPS)	Specifies the coordinates of the field
2.	Envi 5.3	Software for correcting satellite images
3.	ArcGIS 10.4	Coastline digitizing software
4.	Ocean Data View (ODV)	Oceanographic data processing software
5.	Roll Meter	To measure the width of the beach
6.	Geological compasses	To measure the slope of the beach
7.	Ovens	To dry the sediment samples
8.	Sieve Shaker	To separate sediment samples based on the diameter of the sand grains
9.	Digital scales	To weigh the weight of the sediment sample

Table 2. The materials used in this research

No.	Tools	Function
1.	Landsat 8 image data for 2020, 2021 and 2022	As a study resource for mapping changes in the coastline
2.	Data on Lekang Turtle Nests and Eggs in the Eternal Turtle Conservation	As research material
3.	Wind, Wave, Current and Tide Data	As a research parameter
4.	Sand beach	As a research sediment sample

compass is accomplished through dip measurements (Wahyuni *et al*., 2019), which consists of several steps, including attaching the W (west) side of the geological compass body to the ground with the compass arm perpendicular to the strike, adjusting the level of the clinometer tube until the bubble is exactly in the middle with the lever on the compass body, and reading the degree shown on the clinometer.

Sediment Analysis

Trisik Beach sand samples will be collected from each study station and analyzed using the sand fraction method with the Sieve Shaker (Sinulingga *et al*., 2018) to identify the grain size and type of sand. Sand samples will be dried in an oven before being collected from each station for sifting. Sieving was done for 15 minutes. After sieving with a sieve shaker, the products are weighed according to size (Sinulingga *et al*., 2018).

Secondary data for this research was gathered from a variety of linked agencies. The data set comprises spatial and document data, as well as the following: (a). *Wind information.* Wind data from a height of 10 meters will be acquired from the European Center for Medium-Range Weather Forecast (ECMWF) page for the last three years, from 2020 to 2022. The wind components downloaded are zonal wind speed (u) and meridional wind (v). Zonal winds (u) move in an east-west direction, whereas meridional winds (v) move in a south-north direction. (b). *Wave information.* The wave data to be used is the most recent three-year wave data from 2020 to 2022, obtained from the European Center for Medium-Range Weather Forecast (ECMWF) website. The ECMWF global model data can be used without previously executing the process, and the settings are chosen when downloading the file (Fishwaranta, 2017). Significant wave height and mean wave direction are needed components (Saputro, 2010). To obtain rows of data in.txt format, the data format will be transformed using Ocean Data Viewer (ODV) program. (c) *Flow information*. Current data will be acquired from the Copernicus Marine Service (CMS) website for the years 2020-2022, then processed with ArcGIS software to produce current modeling. (d). *Tidal information.* In May 2021, tide data will be obtained from the UNESCO Intergovernmental Oceanographic Commission (IOC) website (http://www.ioc-sealevelmonitoring.org/). The timing is changed based on the accuracy of the available data. It only takes one month of tidal data to determine the type of tide. The data was then analyzed in Microsoft Excel to determine the sorts of ebb and flow. (d). *Data from olive-shelled turtle egg nests and Landsat 8 imagery.* The Eternal Turtle Conservation Group at Trisik Beach provided information about olive ridley turtle nests and eggs. The number of nests, number of turtle eggs, and coordinates of olive ridley turtle nests discovered from 2020 to 2022 are among the data to be collected. The data utilized is Landsat 8 satellite picture data taken from the USGS website (https://earthexplorer.usgs.gov), specifically in 2020, 2021, and 2022.

Data Analysis

Shoreline Change

Digitizing the coastline allows for the detection of changes in the shoreline. Landsat 8 satellite imagery captured using ArcGIS software will be used to process the coastline. Landsat 8 pictures were collected for the years 2020-2022. Each image will be cropped or image cropped, with geometric and radiometric corrections, demarcated or drawn boundaries between land and water, on-screen digitalization, and the Automatic Calculation of Shoreline Changes with Digital Shoreline Analysis System (DSAS) toolbox (Iqbal, 2019).

The delineation between land and sea waters is carried out to clearly describe the boundaries between land and sea, so that the position of the coastline in the image can be seen clearly. Land and sea delineation will use the Modified Normalized Difference Water Index (MNDWI) method, where for Landsat 8 Operational Land Imager (OLI), namely using the formula Ko *et al.* (2015):

$$MNDWI = \frac{Green - SWIR\ 1}{Green + SWIR\ 2}$$

For Landsat 8 OLI, the type of band used is Band 3 Green (0.533–0.590 meter) with a resolution of 30 m and Band 6 SWIR-1 (1.566–1.651 meter) with a resolution of 30 m (Setiani, 2017). For Landsat 8 OLI, the type of band used is Band 3 Green (0.533–0.590 meter) with a resolution of 30 m and Band 6 SWIR-1 (1.566–1.651 meter) with a resolution of 30 meter (Setiani, 2017). (a). *Establishing a Baseline.* The baseline or reference line used to evaluate shoreline changes is created by buffering the earliest coastal data in order to establish a near-ideal baseline (Mutaqin *et al*., 2021). In 2020, the baseline will be established on the mainland (onshore) via the shoreline buffer (Syaharani and Triyatno, 2019). (b). *Shoreline Development.* Shorelines or coasts will be created based on Landsat 8 images taken in 2020, 2021, and 2022. Shorelines or coastlines in 2020, 2021, and 2022 will be created by digitizing the highest tide line seen in satellite photography. (c). *Transect Design.* The transects will face the sea, with a gap of 30 m between them and a length of 500 m (Syaharani and Triyatno, 2019). The distance between the transects is calculated with the premise that each image pixel is represented by one transect (Syaharani, 2019). "Set Default Parameters" automatically makes the transect perpendicular to the baseline.

Coastline change calculations are performed automatically utilizing the DSAS toolbox via "Calculate Statistics" to calculate the distance and rate of shoreline change. Statistical analysis of NSM (net shoreline) and EPR (end point rate) measurements from 2020 to 2022 (2020-2021 and 2021-2022) are included in DSAS measurements. The following formula is used to calculate the statistical analysis of NSM (meters) and EPR (meters/year) (Iqbal, 2019):

NSM = Oldest coastline – Newest coastline

$$EPR = \frac{distance\ between\ oldest\ and\ newest\ coastline\ (meters)}{time\ between\ oldest\ and\ newest\ coastline\ (years)}$$

In addition, for each sample, the coastal area that has changed is calculated (for 2020, 2021, and 2022). This beach area computation is performed using the ArcGIS software's "Calculate Geometry" function. Every year, the coastal area will be estimated from the region that includes the shoreline and baseline.

Processing of Hydro-Oceanographic

Hydro-oceanographic parameters in this study include wind, waves, currents, and tides in the Trisik Beach area. Hydro-oceanographic data that has been obtained will be analyzed through spatial analysis methods using related software. (a). *Wind.* Wind data in the form of a NetCDF file is transformed into.txt format using Ocean Data View (ODV) software so that it may be examined in Ms. Excel (Purwanto *et al*., 2020). Windrose will be characterized depending on the seasons for the last three years by analyzing the *U* and *V* wind speed components. (b). *Wave.* The wave data, which includes major wave heights and the average wave direction, is saved as a Net Common Data File (NetCDF) file, which is then converted to.txt using the Ocean Data View (ODV) program (Rizqiyanto, 2022). The.txt file is then evaluated again and classified based on the direction and height

of the waves in order to create the Waverose model (Saputro, 2010). Waverose modeling is characterized based on the timing of picture alterations along the shoreline throughout the previous three years. (c). *Current.* Using Ocean Data View (ODV) software, stream data in NetCDF format is converted to a text file. The data is then processed in MS Excel to establish the current's speed and direction so that it may be entered into ArcGIS for modeling (Rizqiyanto, 2022). (d). *Tide.* Tidal data will be evaluated using the Admiralty approach to identify the Formzahl value component, allowing the kind of tide to be determined (Mukhtar, 2019). The following formula is used to calculate the Formzahl value:

$$F = \frac{O_1 + K_1}{M_2 + S_2}$$

An explanation of some of the symbols used in determining the Formzahl number is that F is the Formzahl number, O_1 is the amplitude of the main single tidal component caused by the gravitational force of the moon, K_1 is the amplitude of the single main tidal component caused by the gravitational pull of the moon and sun, M_2 is the amplitude of the main double tidal component caused by the gravitational force of the moon, and S_2 is the amplitude of the main double tidal component caused by the gravitational force of the sun. Then, the value of the formzahl number will be categorized according to the characteristics of the tides in the water. The daily semidiurnal tidal type doubles if F is less than 0.25; mixed tides are double dominant if $0.25 < F \leq 1.5$; mixed tides are single dominant if $1.5 < F \leq 3$, and diurnal tides are involved if F is greater than 3 (Suhaemi *et al.*, 2018).

Shoreline Change and the Distribution of Lekang Turtle Nesting

The correlation analysis of shoreline alterations to the distribution of olive ridley turtle nesting in this study used linear regression analysis with SPSS (Statistical Package for the Social Sciences) software (Andriyono and Mubarak, 2011). The findings of the shoreline change data processing will be described in tables or graphs, and then correlated with the number of olive ridley turtle nests and eggs present to determine the relationship between shoreline changes and the distribution of olive ridley turtle eggs. The following is the linear regression equation from X (the independent variable) to Y (the dependent variable):

$$Y = a + bX$$

A definition of the symbols used in the linear regression formula, namely that *Y* represents the number of olive shell nests or eggs, *X* represents the beach area, *a* represents the intercept or constant, and *b* represents the regression coefficient or slope.

RESULTS AND DISCUSSION

Shoreline Change

During 2020, 2021, and 2022, changes in the Trisik shoreline were observed using Landsat 8 OLI data, which was analyzed using ArcGIS and Digital Shorelines Analysis System (DSAS) software. Figure 2, Figure 3, and Figure 4 depicts shoreline alterations that occurred between 2020 and 2022 based on each of the corrected Landsat images. According to Figure 2, Figure 3, and Figure 4, there was a change in the coastal area of Trisik Beach between 2020 and 2022. The three coastlines do not appear to have changed significantly. However, the geographical analysis of each map, which

includes the length of the coastline and annual beach area, reveals significant variances. Table 3 shows the results of the geospatial study of shoreline changes.

Every year, Trisik Beach suffers from abrasion due to a large loss in beach area. Trisik Beach's area will be 537,782.10 m^2 in 2020. Trisik Beach's area decrease to 430,121.80 m2 in 2020 and will further decrease to 425,815.07 m^2 in 2022. According to the findings of this research, Trisik Beach's area decreased by 111,967.03 m^2 between 2020 and 2022. Meanwhile, the length of the Trisik shoreline fluctuates year to year, reaching 5,451.94 m in 2020, 5,454.87 m in 2021, and 5,444.04 m in 2022. The coastline was extended and contracted near the mouth of the Progo River, which is located on the east side of Trisik Beach. The presence of sediment movement is intimately tied to the occurrence of abrasion and accretion events in this estuary. The main source of changes in the shoreline is silt transfer along the coast (Triatmodjo, 1999). Sediment transport along the coast is caused by oceanic processes that present in coastal locations.

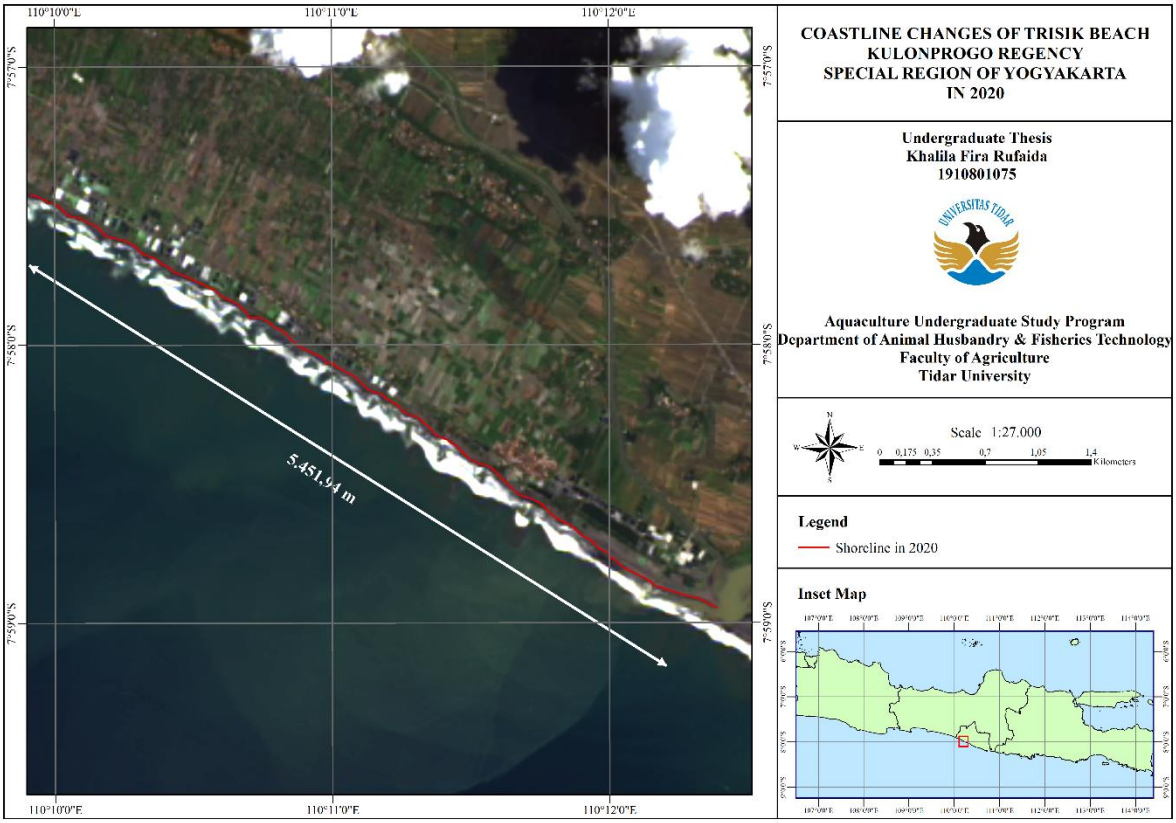

Figure 2. Map of changes in the Trisik coastline in 2020.

Table 3. Changes in the Trisik Coastline in 2020-2022

Year	Coastline Length (m)	Beach area (m^2)
2020	5,451.94	537,782.10
2021	5,454.87	430,121.80
2022	5,444.04	425,815.07

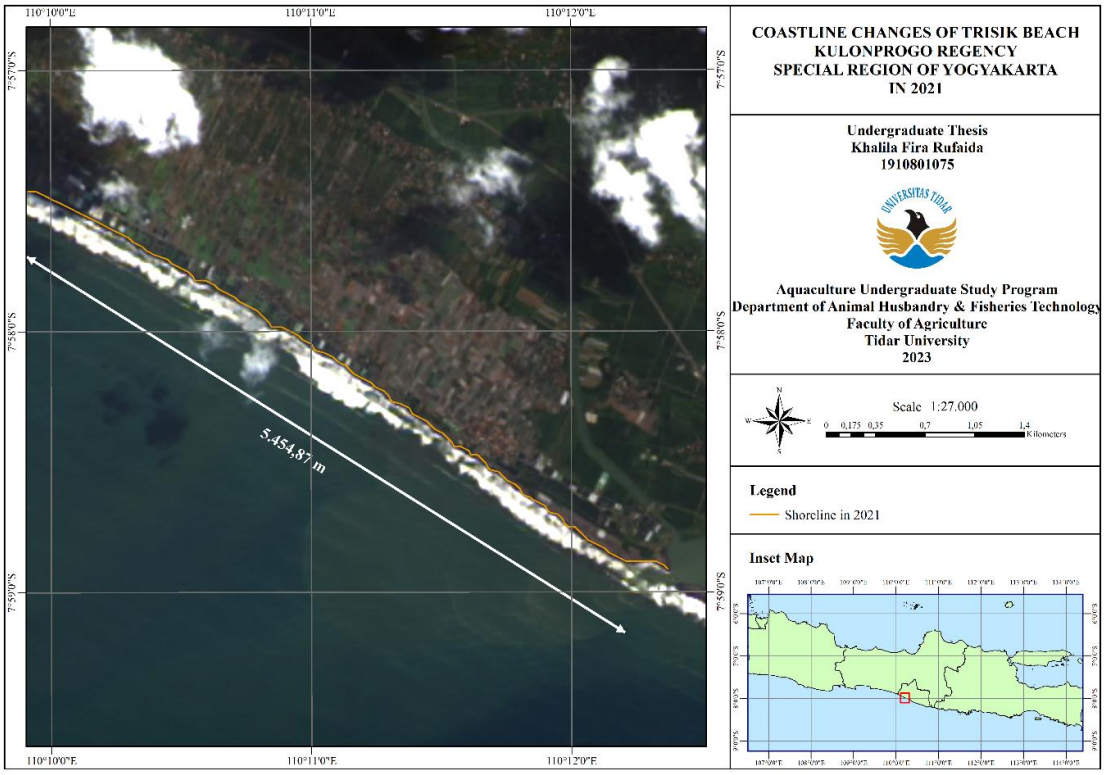

Figure 3. Map of changes in the Trisik coastline in 2021.

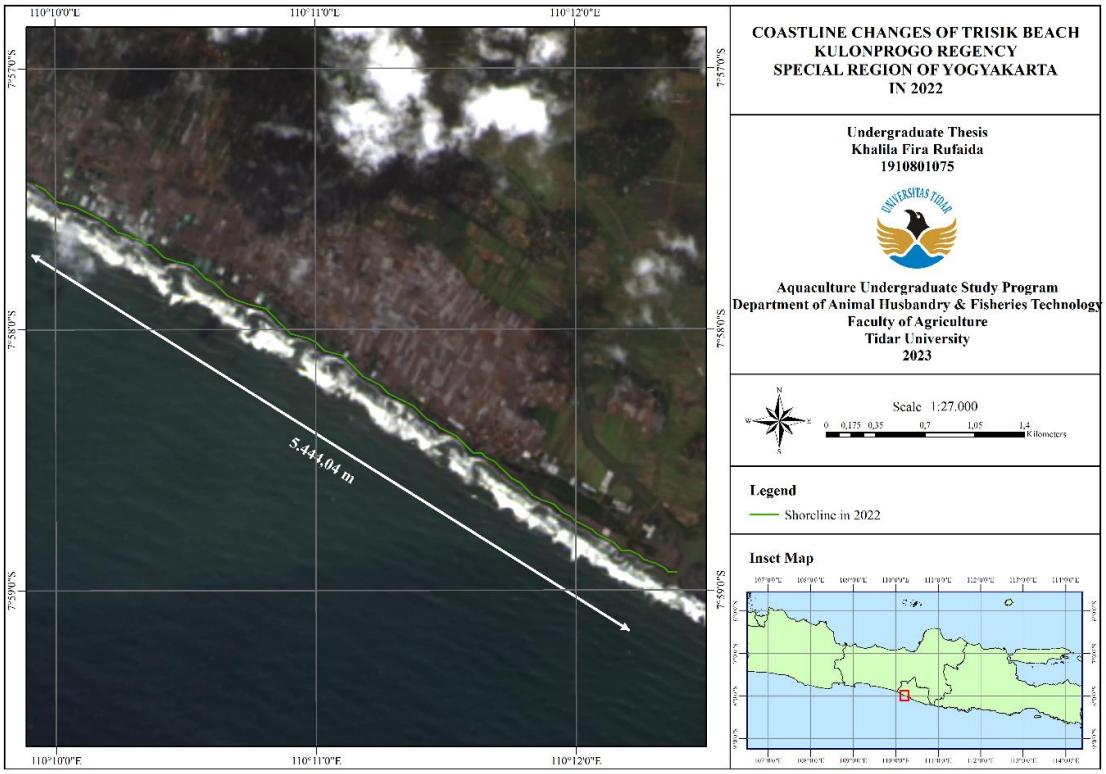

Figure 4. Map of changes in the Trisik coastline in 2022.

Coastline change calculations are also performed using DSAS, a toolbox in the ArcGIS software that aids in the analysis of shoreline changes. Net Shoreline Movement (NSM) analysis is used to compute the distance of change between the oldest and newest shorelines, and End Point Rate (EPR) analysis is used to calculate the rate of change of the coastline by dividing the distance and time. Calculation data has positive (+) and negative (-) values, with positive data (+) indicating accretion and negative data (-) indicating abrasion. Because Trisik Beach goes through two towns, Karangsewu Village and Banaran Village, the coastal region is divided into four areas to make it simpler to examine the changes in the coastline that occurred at Trisik Beach and create more specific data. Figure 5 depicts the division of one hamlet into two regions. NSM and EPR computations are performed automatically on each transect along the coastline using annual shoreline data. Table 4 shows the results of using DSAS to calculate changes in the Trisik coastline from 2020 to 2022.

Table 4. DSAS calculation results for changes in the Trisik coastline for 2020-2022

Area	Location	Net Shoreline Movement (m)			End Point Rate (m/year)		
		Highest	Lowest	Average	Highest	Lowest	Average
A	Karangsewu Village	22.85	-37.70	-15.03	6.38	-10.52	-4.19
B	Karangsewu Village	21.10	-43.14	-16.46	5.89	-12.04	-4.59
C	Banaran Village	0.51	-63.67	-24.59	0.14	-17.77	-6.86
D	Banaran Village	0.75	-62.97	-29.61	0.21	-17.57	-8.26

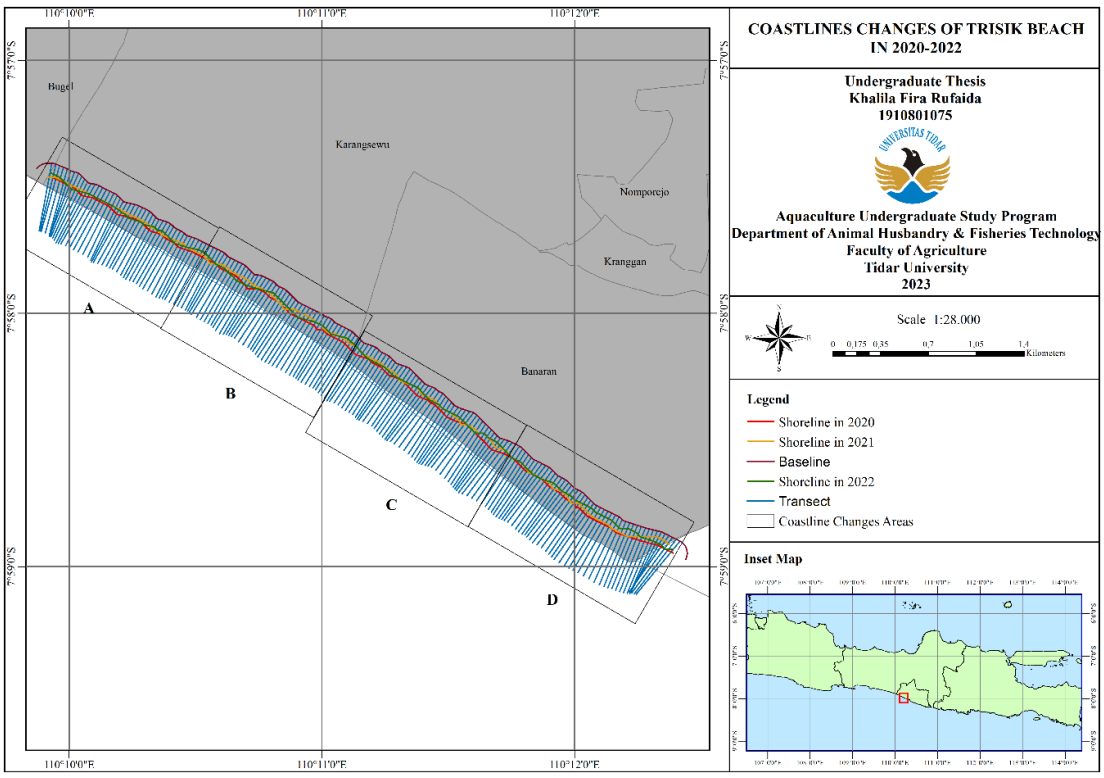

Figure 5. Trisik Coastline Changes Using DSAS.

Based on the results of calculations using the DSAS, it is known that Trisik Beach is experiencing abrasion and accretion. The NSM calculation results in Table 8 show that the average distance for changes in the Trisik coastline is negative (-) in the four areas, namely area A of -15.03, area B of -16.46, area C of -24.59, and area D of -29.61. This shows that Trisik Beach has tended to experience abrasion over the past 3 years. The average abrasion rate shown from the EPR calculation in area A is -4.19 m/year, area B is -4.59 m/year, area C is -6.86 m/year, and area D is -8.26 m/year.

The high level of abrasion on Trisik Beach can be attributed to natural occurrences. Shoreline alterations, both accretion and abrasion, are influenced by variables such as wind, waves, currents, tides, and sedimentation at river mouths (Hanafi, 2005). Because the Special Region of Yogyakarta is directly near to the Indian Ocean, oceanographic influences have a significant impact on the incidence of high shoreline alterations (Cahyono *et al.*, 2017).

Hydro-oceanographic Conditions of Trisik Beach in 2020–2022

The hydro-oceanographic conditions of Trisik Beach, including wind, waves, currents, and tides, were analyzed using spatial analysis methods with remote sensing data from the European Center for Medium Range Weather Forecast (ECMWF) website, Copernicus Marine Service (CMS), and the Intergovernmental Oceanographic Commission of UNESCO (IOC) in the form of time series data collected according to the date of observation data collection for changes in the coastline. The wind rising chart in Figure 6 depicts the findings of wind data analysis in the form of wind direction and speed moving on Trisik Beach in 2020-2022, which are classified by season. The prevailing wind speed on Trisik Beach is 3.6-5.7 m/s of 25.4% in the Western Season, 3.6-5.7 m/s of 21.5% in the Transition I Season, 11.1 m/s of 52.4% in the Eastern Season, and 11.1 m/s of 45.7% in the Transition II Season. While the average wind direction in the West Season is 244.50° from the Southwest, it is 168.74° from the South in the Transitional Season I, 121° from the Southeast in the East Season, and 147.57° from the Southeast in the Transitional Season II, as in Table 5.

According to the percentage of wind speed results, the Trisik Beach region frequently has wind speeds between 3.6 and 5.7 m/s and >11.1 m/s. On the Beaufort Scale, wind speed dominance with a value of 3.6-5.7 in the West Season and Transitional Season I is defined as a sluggish gust. Wind speeds more than 11.1 m/s in the East Season and Transitional Season II are rated as strong winds approaching strong. The formation of waves will be affected by the difference in wind speed. The larger the waves, the longer and stronger the wind blows (Marelsa and Oktaviandra, 2019). The moving monsoon wind influences wind speed and direction due to changes in air pressure in the Northern Hemisphere (BBU) and Southern Hemisphere (BBS) caused by the sun's apparent motion (Rifai *et al*., 2020).

Indonesia, located on the equator, serves as a crossing point for monsoon winds that occur twice a year, notably the West and East Monsoons. The Northern Hemisphere has winter from December to February, while the Southern Hemisphere experiences summer, hence air pressure in the Northern Hemisphere is greater and air pressure in the Southern Hemisphere is lower. As a result, the wind shifts southward from the Asian continent to the Australian continent, where air pressure is lower. The Northwest Monsoon is the wind that blows south, while the East Monsoon blows north between July and August (Surinati and Wijaya, 2017).

The wave rising chart in Figure 7 depicts the findings of wave data analysis in the form of significant wave heights and the direction of waves flowing on Trisik Beach in 2020-2022, which are classified by

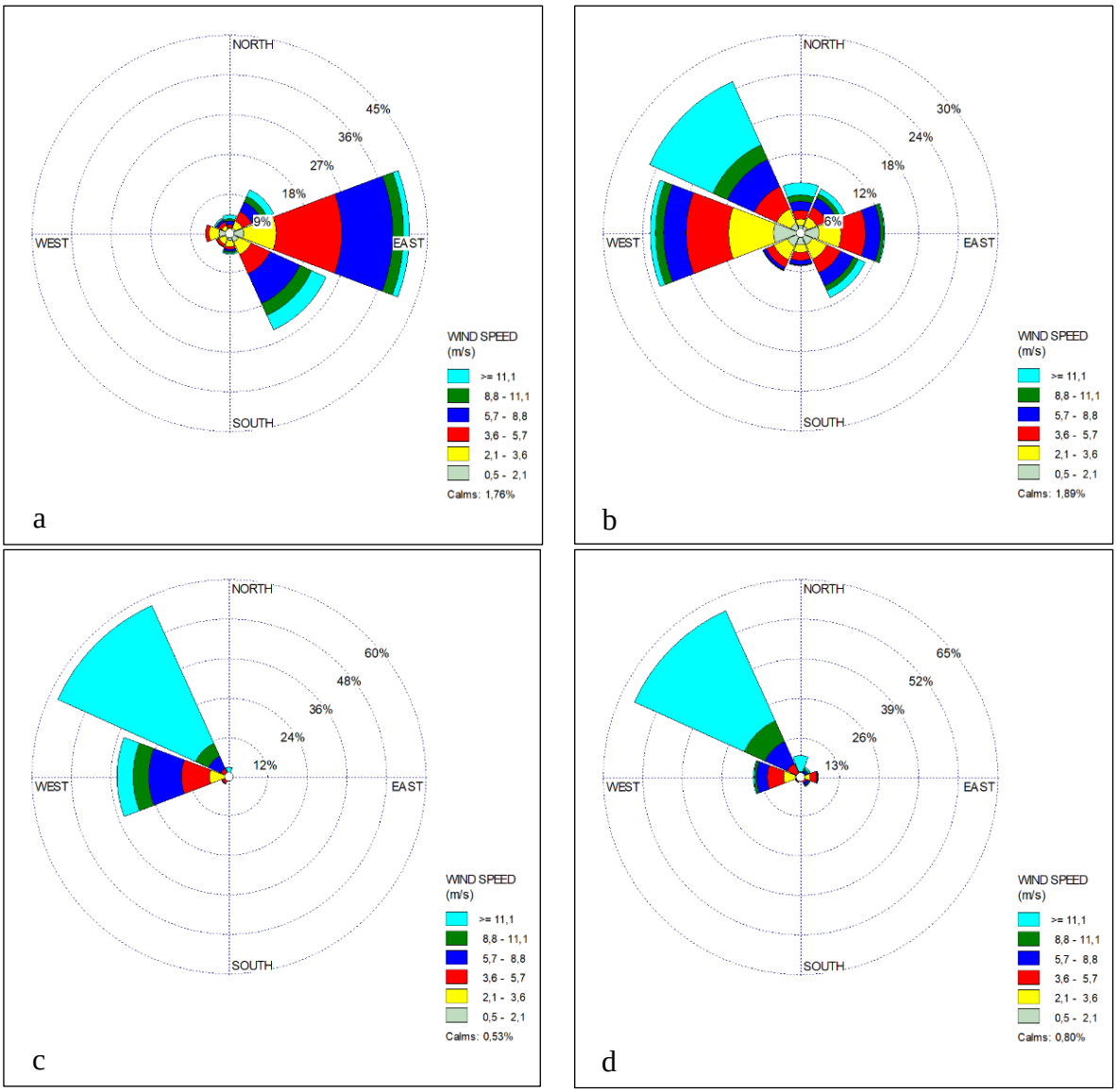

Figure 6. Wind Direction and Speed. a) The West Monsoon, b). In Transitional Season I, c). In the east monsoon, d). In the transitional season II.

Table 5. Wind speed and direction

Season	Wind Speed (m/s)	Wind Direction (degree)
Western season	5.47	244.5
Transition Season 1	6.28	168.74
Eastern Season	14.94	121
Transition Season 2	14.10	147.57

season. Figure 7a depicts the dominating wave in the west season, with wave heights ranging from 0.5 to 2.1 m. The primary wave in the east monsoon is travelling north, as indicated in Figure 7c, with a wave height of 2.1-3.6 m. In the Transition II season, the primary waves are going north with a wave height of 0.5-2.1 m, as seen in Figure 7d, as in Table 6.

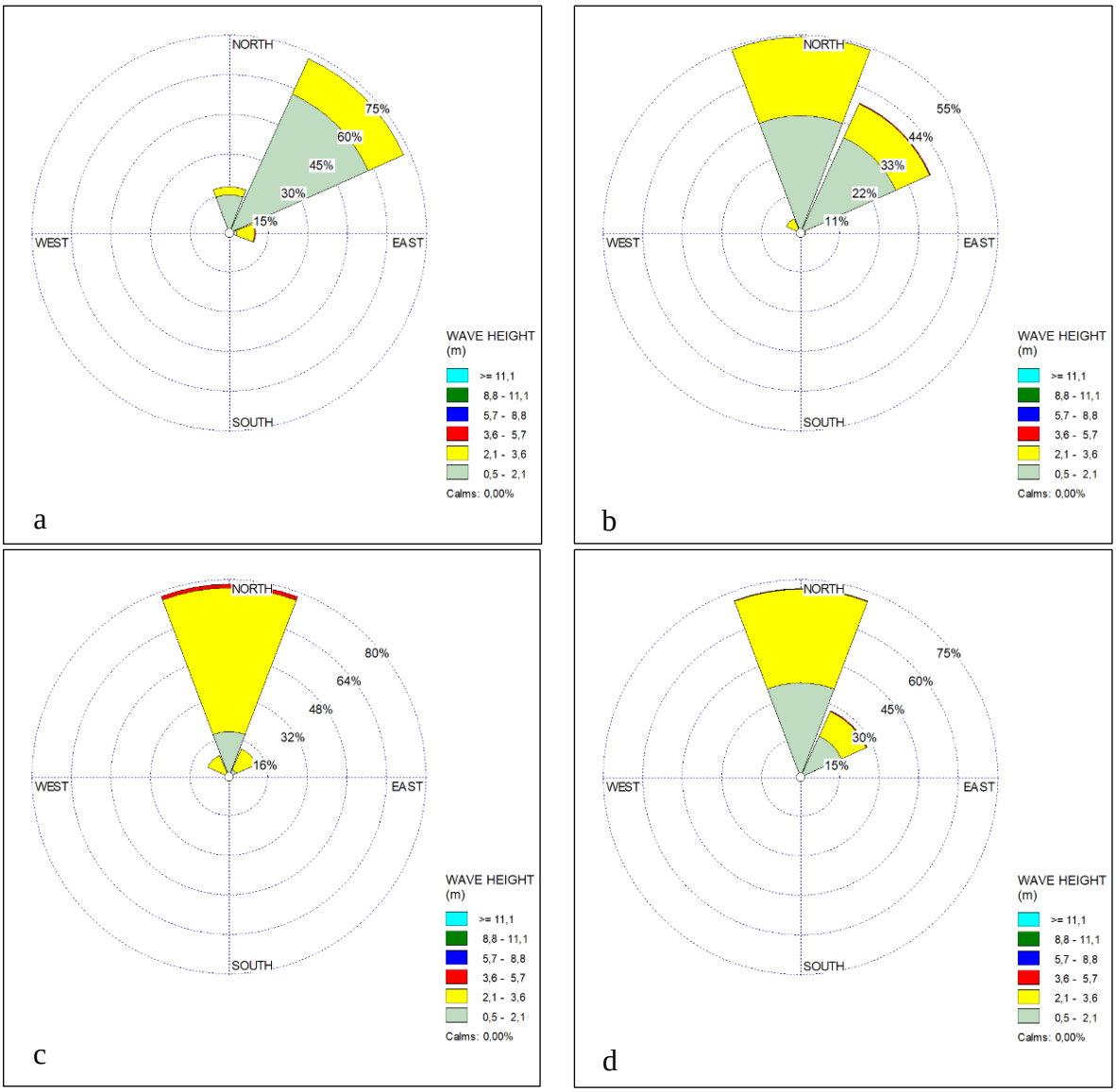

Figure 7. a). Direction And Speed of Sea Waves. A) The West Monsoon, b). In Transitional Season I, c). In the east monsoon, d). In the transitional season II.

Table 6. Wave hight and direction

Season	Wave Hight (m)	Wave Direction (degree)
Western season	1.85	220.54
Transition Season 1	1.95	198.25
Eastern Season	2.42	183.75
Transition Season 2	2.07	195.02

In general, the waves on Trisik Beach have a height dominated by 0.5-2.1 m, followed by 2.1-3.6 m, and the largest wave height on Trisik Beach is 3.-5.7 m. This demonstrates that the waves on Trisik shore are destructive or cause damage to the shore since they are taller than 1 m (Rini, 2022). These powerful waves can erode beach sand,

resulting in steep coastal areas (Tyas and Dibyosaputro, 2012). The large waves that travel towards the beach take beach sediment back to the sea, causing the beach height to fall. In general, sea waves are caused by wind on the water's surface. As a result, the waves exhibit wind-influenced qualities, such as the higher the speed of the wind blowing in a canal, the larger the speed and length of the sea waves (Azis, 2006).

The CMS page current data comes in the form of surface geostrophic current data for 2020-2022, which is examined to determine the average current per season. Figure 8 depicts the findings of an examination of ocean currents along the south shore of the Special Region of Yogyakarta. The pattern of current movement in the West Season that happened between 2020-2022 is mainly towards the east, with a current speed of 0.04-0.34 m/s. With a current speed of 0.04-0.46 m/s, the pattern of current travel in Transitional Season I is east in the coastal area and northwest in the middle of the ocean. During the East Season, the pattern of current travel is eastward in the coastal area and westward elsewhere. The sea is in the middle of the ocean and to the northwest with a current speed of 0.04-0.52 m/s, whereas in the Second Transitional Season the pattern of current movement is generally to the east with a current speed of 0.04-0.58 m/s and strong currents in the oceanside area.

The movement of monsoon winds that emerge across the southern waters of Java and Bali, resulting in a seasonal reversal of wind direction, might alter the pattern of surface currents on the south coast of DI Yogyakarta (Surinati and Wijaya, 2017). According to the wind rose chart for 2020-2022, this can be observed in the middle of the ocean, where the pattern of current directions follows the movement of the wind in the waters. The wind's movement will supply kinetic energy and push the water on the sea surface in the direction of the wind, but due to the influence of the Coriolis force on the sea surface, the direction of current motion is deflected by 45° from the wind direction (Sari *et al*., 2020).

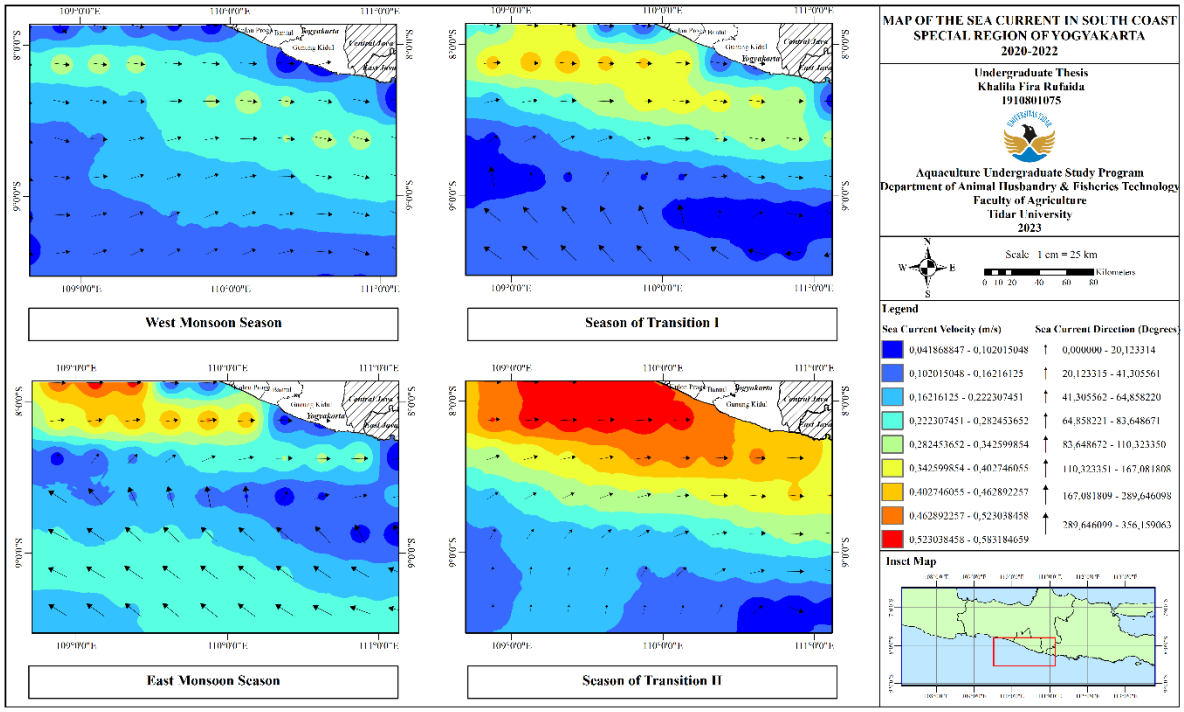

Figure 8. Seasonal current distribution map on Trisik Beach.

It is demonstrated in Transition Season I, East Season, and Transition Seas'n II that the current speed at the ocean's edge is faster than the current speed in the middle of the ocean. This is due to the effect of the Java Coastal Current (APJ), which carries a mass flow of surface water to the southeast along Sumatra's southwest coast and eastward along Java's south coast to Sumbawa (Mbay and Nurjaya, 2011). The presence of the APJ causes water masses to accumulate in the southern waters of Java Island's western and central regions, while water masses remain low in the eastern part (Dimas *et al*., 2015). According to Marpaung and Harsanugraha (2014), the accumulation of water masses on the ocean's edge causes the speed of surface currents to be faster at the ocean's edge than in the centre of the ocean.

Eddy currents are caused by the presence of a circular current pattern in the middle of the ocean, as depicted in the figure 8. Eddy currents are circular currents with spatial sizes of tens to hundreds of kilometers and temporal periods of weeks to months (Nuzula *et al*., 2016). Depending on the direction of the vortex and the position of the vortex formation, an eddy can cause upwelling or downwelling. Cyclic eddies create upwelling in the Southern Hemisphere, while anticyclonic eddies form downwelling (Pranowo *et al*., 2016).

From May 2, 2021 to May 30, 2021, the tides on Trisik Beach are processed using tidal data from the IOC tide data provider website. The data collecting schedule is based on the most recent 30 days of tide data available on the IOC website. Table 7 shows the results of tidal data analysis using the Admiralty approach, which yields amplitude harmonic constants (A) and phase values (g).

Based on the calculation of the Formahzl (F) number, the F value is 0.38, which means that the mixed tidal type tends to be mixed daily (mixed semidiurnal), where O1 is the amplitude of the main single tidal component caused by the gravitational force of the moon, K1 is the amplitude of the single main tidal component caused by the gravitational pull of the moon and sun, M2 is the amplitude of the main double tidal component caused by the gravitational force of the moon, and S2 is the amplitude of the main double tidal component caused by the gravitational force of the sun. Mixed tides have two highs and two lows with different intervals in a single day. This sort of tide is consistent with Triatmodjo's (1999) tidal distribution chart, which shows that the south coast of Java Island has mixed-type tides that tend to double daily. According to Wyrrtki (1961) and Pariwono (1989), double daily tides can be seen in Indonesian territory in the Malacca Strait and the Indian Ocean (Ichsari *et al*., 2020). The types of tides that exist in a body of water can have an impact on the abrasion and sedimentation processes that occur there. When compared to water areas with a single daily ebb, water areas with numerous daily mixed ebbs and flows have a more dynamic sediment transport process (Daulay, 2014).

Relationship Between Hydro-Oceanographic Conditions and Trisik Shoreline Change

According to an analysis of hydro-oceanographic conditions in the Trisik Beach area over the last three years, winds in the Trisik Beach area, as shown in Figure 6, tend to be strong during the East Season

Table 7. Tidal harmonic constant results

	M2	S2	N2	K2	K1	O1	P1	M4	MS4
A (cm)	52.40	29.65	9.84	6.82	19.18	12.08	6.33	1.14	0.96
g	233	300	205	300	270	251	270	201	80

(June-August) and the Second Transitional Season (September-November). Higher waves and faster currents are generated by these strong winds than during the West Season (December-February) and Transitional Season I (March-May) The direction of the current in Figure 8 is also linear with the seasonal shift of the wind direction. The wind comes from the Southwest (244.50°) and the current flows to the East (94.11°) in the West Season, whereas the wind comes from the Southeast (121°) and the current moves to the Northwest (298, 62°) in the East Season. However, because of the Java Coastal Current (APJ) and the accumulation of seawater masses, the longshore currents, as shown in Figure 8, travel to the east and are moving at a rather quick speed. Furthermore, the waves at Trisik Beach (Figure 7) average 1 m in height and feature mixed tides are double dominant (F = 0.38). The hydro-oceanographic dynamics, which are rather intense and occur on a continual basis, have caused shoreline modifications at Trisik Beach due to excessive sediment movement during the oceanographic process. Waves, tides, ocean currents, and longshore currents influence the majority of sediment transport in coastal locations (Triyatno, 2014).

Longshore currents cause silt to be transported by seawater, resulting in sediment movement and changes on beaches. In addition to the relatively destructive wave heights, the beach undergoes abrasion from high waves, and the presence of high tides twice a day causes beach sediments to be eroded by sea water more regularly. This sediment transfer is visible in changes to the coastline in 2021, when the Trisik coastline is longer than it was in 2020 and 2022. The shoreline lengthens in the east, where sand deposits concentrate near the mouth of the Progo River, making the mouth of the Progo River appear narrower. Furthermore, coastal abrasion has caused a decline in the coastline over the last three years, as evidenced by the results of calculating the distance and the average abrasion rate (Table 4), which show that the highest average distance to change the coastline (NSM) is -29.61 m, the lowest is -15.03 m, and the highest average abrasion rate (EPR) is -8.26 m/year and the lowest is -4.19 m/year. Trisik Beach's area shrank by 111,967.03 m2 between 2020 and 2022.

Distribution of Lekang Turtle Nests on Trisik Beach

Olive ridley turtles prefer beaches like Trisik Beach in Kulonprogo Regency as a place to nest. At Trisik Beach, residents regularly find nests of olive ridley turtles, complete with eggs. With the help of the local community, the Abadi Turtle Conservation Group gathered and documented nesting and nesting data for olive ridley turtles residing on Trisik Beach. The quantity of olive ridley turtle nests and eggs found on Trisik Beach between 2020 and 2022 is displayed in Table 8. According to statistics from the Abadi Turtle Conservation Group on olive ridley turtle nests and nesting habits, there will be less nests and eggs in the general vicinity of Trisik Beach in 2020, 2021, and 2022. There will be 58, 28, and 13 nests, respectively, in 2020, 2021, and 2022, with 5189, 2711, and 1224 eggs. Olive ridley turtle nests have been discovered in several locations at Trisik Beach. This is due to the beach's characteristics. The bio-physical parameters of the beach, such as beach width, beach slope, sand percentage, sand temperature, light intensity, food availability, and beach vegetation, all influence turtle landings on the beach (Cao *et al.*, 2017).

Figure 9 shows the distribution of data on the location of olive ridley turtle nests on Trisik Beach in 2021, along with their coordinate coordinates. Based on data acquired from the olive ridley turtle nests and eggs of the Abadi Turtle Conservation Group, 58 nests were located in 2021, distributed in groups at the position points illustrated in Figure 9. Because of the large

Table 8. Number of nests and eggs of olive ridley turtles

Year	Discovery of the Nest												Total Nest	Total Eggs
	Jan	Feb	Mar	Apr	Mei	Jun	Jul	Aug	Sep	Okt	Nov	Des		
2020	-	-	-	3	4	12	21	13	2	3	-	-	58	5189
2021	-	-	-	1	7	13	7	-	-	-	-	-	28	2711
2022	-	-	-	5	6	2	-	-	-	-	-	-	13	1224

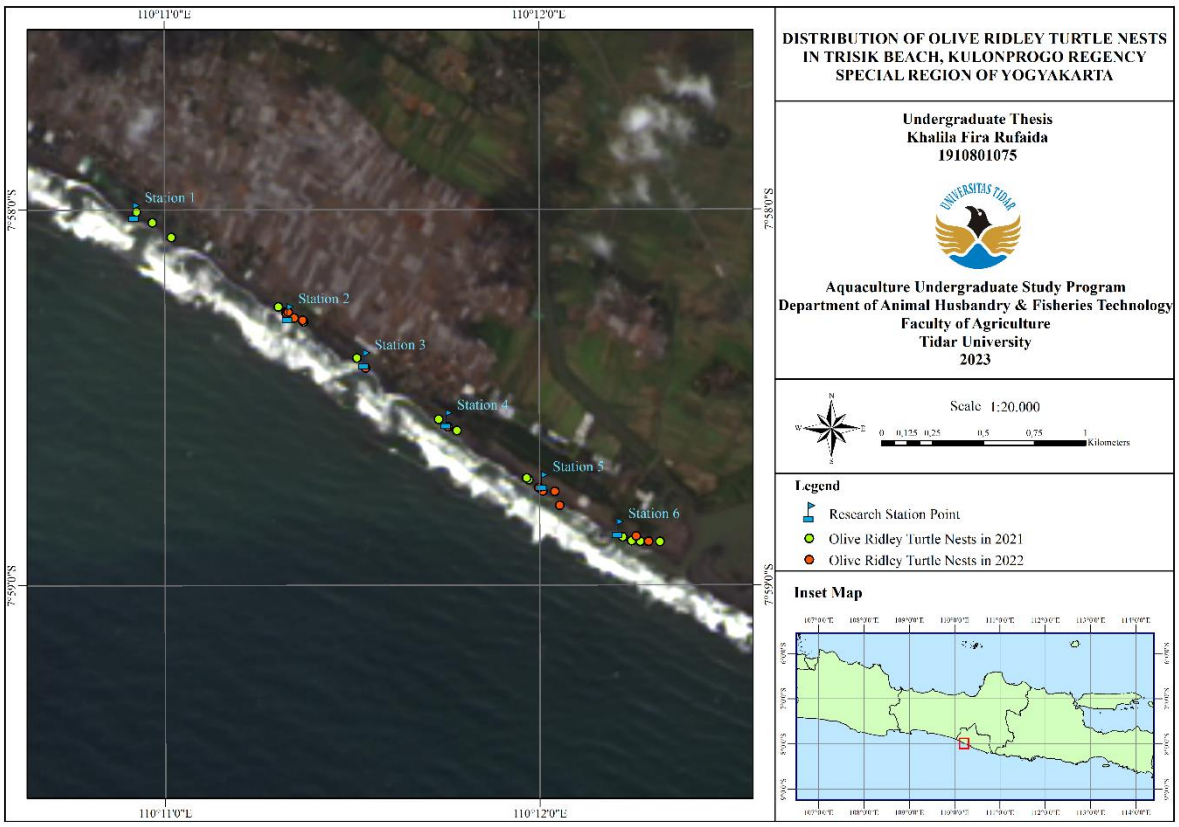

Figure 9. Map of Distribution of Lekang Turtle Nests In 2021.

number of nests discovered there, the six places are thought to be popular spots for olive ridley turtles to lay their eggs. The six location points for further investigation of the olive ridley turtle nesting habitat at Trisik Beach were chosen.

Characteristics of the Lekang Turtle Nesting Habitat

Coastal morphology is vital for turtles in choosing ideal places for nesting and laying eggs. This relates to the possibility of hatchability being generated in a location so that turtles will return there. The width of the beach, the slope of the beach, and the type of sand are all physical aspects of the morphology of the shape of the beach chosen by turtles in deciding the place used as nesting habitat. Table 9 shows the findings of measuring the width and slope of Trisik Beach at the six research locations.

The findings of measuring the beach width show that the width of the beach at Trisik Beach ranges from 11 to 30.48 meters, with an average beach width of 20.16 meters. The recommended beach width for turtle nesting is 30-80 meters (Nuitja, 1992).

Station 5 is a good nesting habitat since it has a beach width greater than 30 m, whereas the other five stations have a beach width less than 30 m. Based on field investigations, stations with a beach width of less than 30 m nevertheless have enough distance from the highest tide to the outermost vegetation barrier, ensuring that nesting grounds are protected from seawater inundation. The breadth of the beach utilized as nesting habitat has a significant impact on the ability of olive ridley turtles to reach nesting locations (Septiadi, 2018). Furthermore, if the nest is located far enough away from the tidal area, the failure of hatching turtle eggs caused by turtle nest submergence can be avoided (Nuitja, 1992).

The slope of the coast of Trisik Beach ranges from 10 to 45 degrees, with an average slope of 20.67 degrees. In general, Trisik Beach has a favorable beach slope for turtle nesting because turtles prefer nesting places with less than a 30° slope (Witherington et al., 2003). Stations 1, 2, 3, 4, and 6 have a beach slope of less than 30° and are categorized as steep, however station 5 has a beach slope of more than 30° and is rated as extremely steep, making it unsuitable for turtles. The slope of this beach has a significant impact on turtles' access to ideal sites for laying eggs. Turtles can only see properly from a vantage point of 150°, so the steeper the coast, the more difficult it will be for turtles to perceive distant objects (Septiadi, 2018). If the coast becomes steeper, the energy expended by the turtles to climb up and lay their eggs will increase, causing the mother turtles to get exhausted before reaching the nesting spot. Mother turtles use a lot of energy and are more prone to disturbance while nesting on coastal plains with sloping and wide morphology (Horrocks and Scott, 1991).

Along the coast of Trisik Beach, there is silt in the form of black sand. The size distribution of the sand sediments found at each site was studied and categorised using a sieve shaker. Figure 10 depicts the findings of the investigation of the distribution of sand types, which show that fine sand (0.10-0.21 mm) dominates each station with varied percentages, namely 65.15-94.86%. The characteristics of these sediments indicate that the sediments at Trisik Beach are suitable for turtle nesting, in accordance with Bustard's (1972) opinion that fine sand (0.10-0.21 mm) and medium sand (0.21-0.50 mm) are suitable for turtle nesting habitat (Nasiti and Sunarto, 2017). Turtles prefer fine sand with a sediment content of around 90% in the form of 0.18-0.21 mm sand, with the remaining being silt and clay (Nuitja,

Table 9. Width and slope of Trisik Beach

Station	Coordinate	Beach Width (m)	Beach slope	
			Degrees (°)	Characteristics
1	S 07°58'00.3" E 110°10'55.3"	23,46	10	Steep
2	S 07°58'16.5" E 110°11'19.9"	18,28	15	Steep
3	S 07°58'23.9" E 110°11'32.1"	12,83	17	Steep
4	S 07°58'33.5" E 110°11'45.3"	30,48	24	Steep
5	S 07°58'43.4" E 110°12'00.6"	11	45	Very Steep
6	S 07°58'50.9" E 110°12'12.7"	24,9	13	Steep

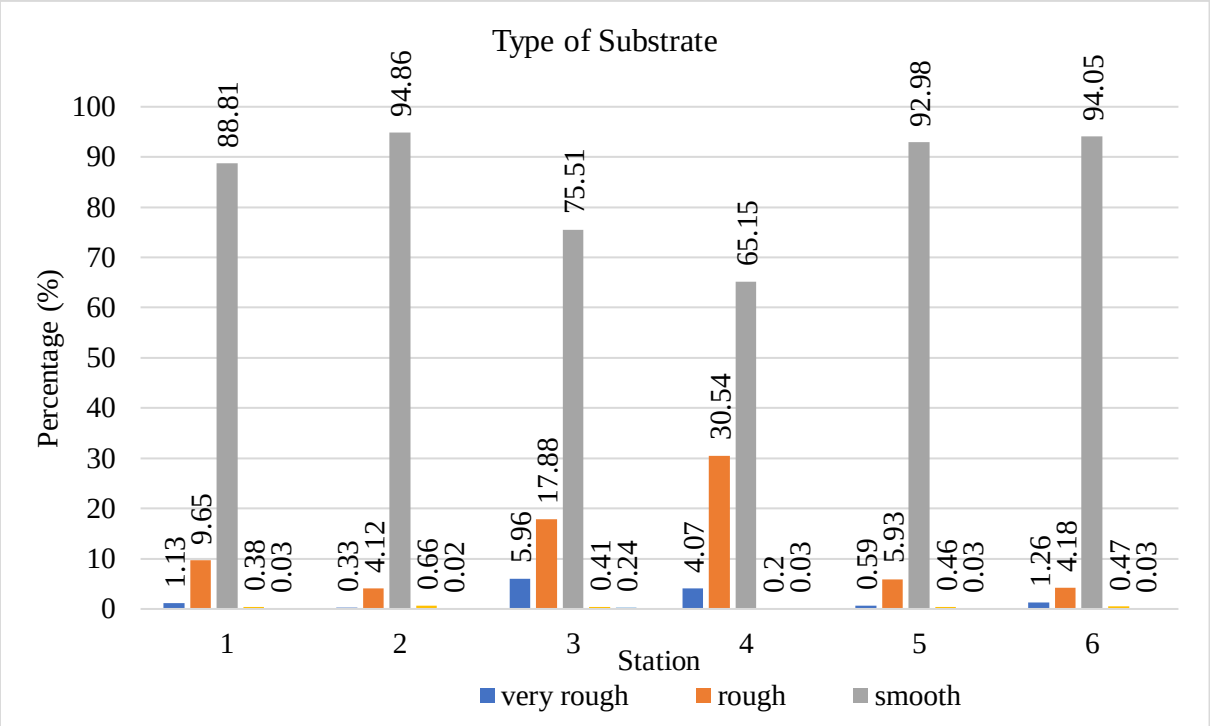

Figure 10. Percentage of grain size of sand sediments.

1992). Stations 2, 5, and 6 have fine sand content of more than 90%, making them ideal for turtle nesting places. The other three stations, namely station 1, station 3, and station 4, have a fine sand proportion of less than 90%.

Sand's grain size influences its ability to act as a good temperature buffer (Nybakken, 2005). Furthermore, because black sand contains a high mineral content, it has the potential to absorb and maintain a steady temperature in the sand when compared to white sand (Rofiah *et al.*, 2012). Black beach sand can absorb up to 80% of incoming heat radiation and minimize evaporation from the sand's surface (Sears and Zemansky, 1982).

Changes in the Trisik Shoreline and the Distribution of Lekang Turtle Nesting

The dynamics of ongoing changes in the shoreline at Trisik Beach have affected the beach area from 2020 to 2022. Trisik Beach has suffered a substantial deterioration during the last three years. This causes the morphology of the beach to alter throughout the year. These alterations have an indirect impact on the distribution of olive ridley turtle eggs on Trisik Beach. According to the results of the regression analysis between the beach area and the number of olive ridley turtle nests shown in Figure 11, the number of nests found each year is directly proportional to the beach area, with a decreasing beach area resulting in a decreasing number of olive ridley turtle nests. The derived linear regression equation is Y = -127.33+ 0.0003 X, with a correlation value (R) of 0.955 and a coefficient of determination (R2) of 0.913. The negative constant value (intercept) signifies that if the beach area score (X) is regarded non-existent or equal to 0 (zero), the point of intersection of the lines is at the score for the number of olive shell nests (Y), which has a value of -127. This means that if the beach area is reduced to nothing, the number of olive ridley turtle nests detected on Trisik Beach will drop until a total of 127 nests are lost. Constants with negative values occur

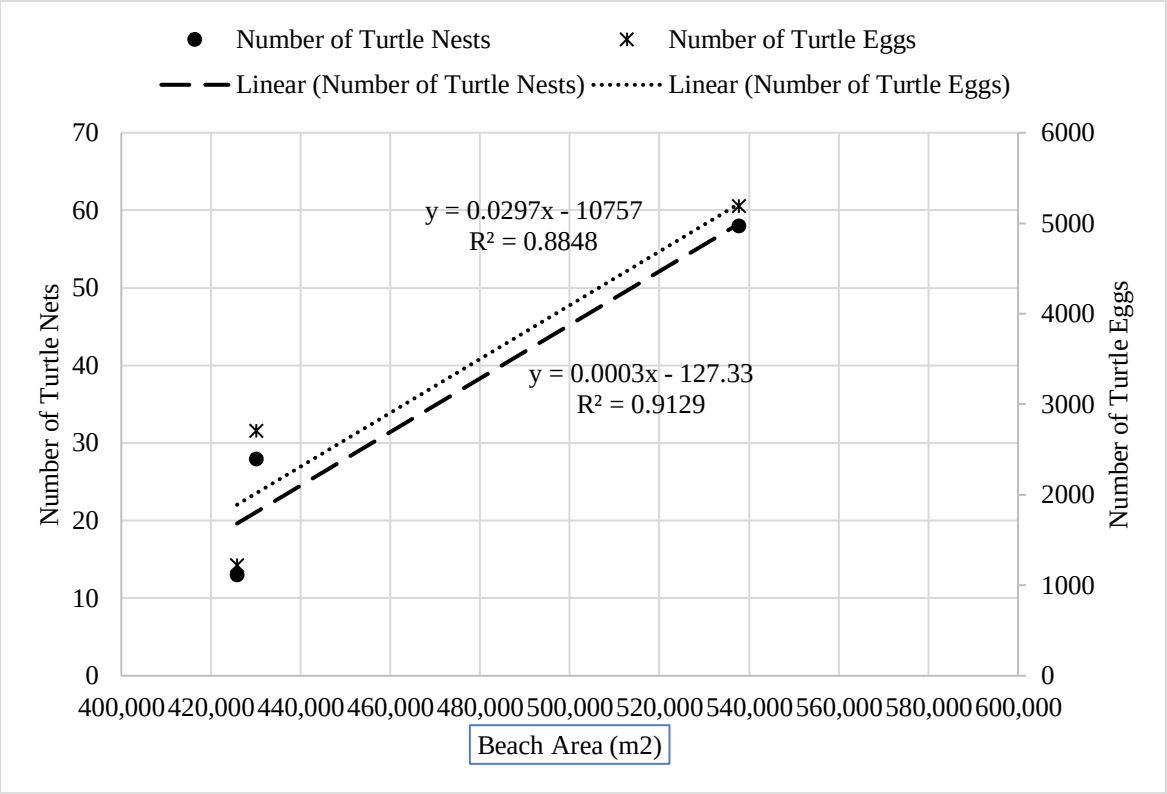

Figure 11. The Relationship Between Beach Area and The Number of Turtle Nets and Turtle Eggs.

when the range between the independent variable (X) and the dependent variable (Y) is large enough (Dougherty, 2002). The beach area variable has a unidirectional positive relationship to the number of olive ridley turtle nests, as indicated by the positive regression coefficient of 0.0003; this means that increasing the beach area score will increase the number of olive ridley turtle nests found, and vice versa. According to the coefficient of determination, the relationship between beach area and the number of olive ridley turtle nests observed has a very good correlation (r = 0.955; 0.75 < r < = 0.99), with the beach area influencing the number of turtle nests by 91.3%. The relationship between beach area and the number of olive ridley turtle nests is shown in the Figure 11.

According to the results of the regression analysis between the beach area and the number of olive ridley turtle eggs shown in Figure 11, the number of eggs found is directly proportional to the beach area each year, with decreasing beach area causing a decrease in the number of olive ridley turtle eggs. The linear regression equation for the number of olive ridley turtle eggs obtained is Y = -10756.53+0.0297X, with a correlation value (R) of 0.941 and a coefficient of determination (R2) of 0.885. The negative constant value (intercept) indicates that if the beach area score (X) is considered non-existent or equal to 0 (zero), the point of intersection of the lines is at the olive ridley turtle egg number score (Y) with a value of -10757, implying that if the area score (X) is considered non-existent or equal to 0 (zero), the point of intersection of the lines is at the olive ridley turtle egg number score (Y) with a value The quantity of olive ridley turtle eggs found on Trisik Beach will diminish until there are none, resulting in a potential loss of 10,757 eggs. The positive regression coefficient for beach area of 0.030 indicates that the beach area variable is related to the number of olive ridley turtle eggs in the same direction; this means that increasing the beach area score will increase the number of olive ridley turtle eggs found, and

vice versa. The association between the beach area and the number of olive ridley turtle eggs was discovered to have a very good correlation ($r = 0.885$; $0.75 < r < 0.99$), with a percentage of 88.5% that the number of turtle eggs is impacted by the beach area.

The reduction in beach area of 111,967.03 m^2 in the last three years has significantly reduced the number of nests and eggs for olive ridley turtles. The retreating coastline as a result of extreme oceanographic influences has an impact on changes in the morphology of the coast, so this will be a very crucial threat to sea turtles. The threat of habitat loss for the olive ridley turtle on Trisik Beach can be seen from the reduced slope and width of the beach used as a nesting area. Most of the width of Trisik Beach is not suitable for turtle habitat, while the slope of the beach is still quite ideal. However, if the influence of oceanography continues and abrasion occurs, the slope of the beach may become steeper, making it less suitable for turtle habitats.

Decreasing the width of the beach and the slope of the beach will reduce the number of nests and eggs found for olive ridley turtles because olive ridley turtles have a preference for nesting in certain areas that are different from other turtle species. The olive ridley turtle shows a strong preference for nesting as far away from the highest tide line as possible (Avila-Aguilar, 2015). The choice of nesting sites away from the highest tides indicates that the olive ridley turtle's main priority is protecting the nest from tidal inundation. This is done to avoid the infiltration of salt water into turtle eggs (Mustaqim *et al*., 2020), because the salt content in seawater in the nest environment can trigger an osmotic imbalance in the eggs so that the eggs will experience water loss and affect hatching success (Sifuentes-Romero *et al*., 2018). In addition, female turtles will nest with attention to balance by finding a safe elevation or height and expending the energy used in crawling to that place, where they will not crawl any farther than necessary (Maurer and Johnson, 2017). Abrasion also affects changes in the percentage of sand types, but changes in the percentage of sand do not have a major effect on turtle landings as long as the width and slope of the beach are still ideal (Mustaqim *et al*., 2020).

CONCLUSION

Based on the results of the analysis and discussion in this research, it can be concluded that: (1) Coastline changes that occur at Trisik Beach during 2020-2022 tend to experience erosion due to the decreasing beach area; the highest average distance value of shoreline changes is -29.61 m; the lowest is -15.03 m; and the average value is The highest average abrasion rate was -8.26 m/year, while the lowest was -4.19 m/year, resulting in a coastal area reduction of 111,967.03 m^2. (2) The association between changes in the coastline and the distribution of olive ridley turtle nesting at Trisik Beach is quite significant, with the beach area influencing 91.3% of the number of turtle nests and 88.5% of the number of turtle eggs.

REFERENCES

Andriyono, S., and Mubarak, A. S. 2011. Korelasi Perubahan Garis Pantai Terhadap Konservasi Penyu Hijau (*Chelonia mydas*) Di Taman Nasional Meru Betiri, Jawa Timur. *Jurnal Ilmiah Perikanan dan Kelautan*, 3(2): 139-144.

Ávila-Aguilar, A. 2015. Nest-site selection of Lepidochelys olivacea (Testudines: Cheloniidae) in the South Pacific region of Costa Rica. *Revista de biología tropical*, 63: 375-381.

Azis, M.F. 2006. Gerak air di laut. *Oseana*, 31(4): 9-21.

Cahyono, H., Retno, T., Musrifah, W. and Maulana, E. 2017. Analisis Perubahan Garis Pantai dengan Menggunakan Data Citra Landsat di Pesisir

Kabupaten Kulonprogo. Parangtritis Geomaritime Science Park, 2.

Cao, W., Li, R., Chi, X., Chen, N., Chen, J., Zhang, H. and Zhang, F. 2017. Island urbanization and its ecological consequences: A case study in the Zhoushan Island, East China. *Ecological Indicators*, 76: 1-14.

Daulay, A.B. 2014. *Karakteristik Sedimen Di Perairan Sungai Carang Kota Rebah Kota Tanjungpinang Provinsi Kepulauan Riau. Tanjungpinang*. Skripsi. Universitas Maritim Raja Ali Haji

Dimas, R., Setiyono, H., dan Helmi, M. 2015. Arus Geostropik Permukaan Musiman Berdasarkan Data Satelit Altimetri Tahun 2012-2013 Di Samudera Hindia Bagian Timur. *Jurnal Oseanografi*, 4 (4): 756 – 764

Dougherty, C. 2011. *Introduction To Econometrics*. Oxford University Press. New York.

Fishwaranta, A., Wida, D. A. K., dan Fachrurrozi, M. 2017. Pemanfaatan Data Model Global, Citra Satelit, Dan Data Observasi Udara Atas Untuk Identifikasi Kejadian Puting Beliung Dan Waterspout Di Kupang–NTT. *Jurnal Meteorologi Klimatologi dan Geofisika*, 4(2): 1-6.

Hanafi, M. 2005. Hubungan Faktor Perilaku Manusia, Faktor Alam Dengan Perubahan Garis Pantai Untuk Optimisasi Pengelolaan Wilayah Pesisir Di Kabupaten Indramayu Jawa Barat

Harsiti, Muttaqin, Z., and Srihartini, E. 2022. Penerapan Metode Regresi Linier Sederhana Untuk Prediksi Persediaan Obat Jenis Tablet. *JSiI (Jurnal Sistem Informasi)*, 9(1): 12-16.

Hartri, A., Sudarsono, B., and Awaluddin, M. 2015. Analisis Dampak Perubahan Garis Pantai Terhadap Batas Pengelolaan Wilayah Laut Daerah Istimewa Yogyakarta. *Jurnal Geodesi Undip*, 4(4): 316-324.

Horrocks, J.A. and Scott, N.M. 1991. *Nest site location and nest success in the hawksbill turtle Eretmochelys imbricata in Barbados, West Indies*. Marine Ecology Progress Series, hlm 1-8.

Ichsari, L.F., Handoyo, G., Setiyono, H., Ismanto, A., Marwoto, J., Yusuf, M. and Rifai, A. 2020. Studi Komparasi Hasil Pengolahan Pasang Surut Dengan 3 Metode (Admiralty, Least Square Dan Fast Fourier Transform) Di Pelabuhan Malahayati, Banda Aceh. Indonesian *Journal of Oceanography*, 2(2): 121-128.

Iqbal, A. M. 2019. *Deteksi Perubahan Garis Pantai Di Wilayah Pantai Jabon, Kabupaten Sidoarjo Menggunakan Digital Shoreline Analysis System (DSAS)*. Disertasi. Universitas Brawijaya.

Ismail, N.P., 2017. Dinamika Perubahan Garis Pantai Pekalongan dan Batang, Jawa Tengah.

[MMAF] Ministry Of Marine Affairs And Fisheries. 2009. Pedoman Teknis Pengelolaan Konservasi Penyu. Direktorat Konservasi dan Taman Nasional Laut, Direktorat Jenderal Kelautan, Pesisir dan Pulau-Pulau Kecil, Departemen Kelautan dan Perikanan. Jakarta. 123hlm.

[MMAF] Ministry of Marine Affairs and Fisheries. 2010. Rencana Strategi Kementerian Kelautan dan Perikanan 2010-2014. Kementerian Kelautan dan Perikanan. Jakarta.

[MMAF] Ministry of Marine Affairs and Fisheries. 2015. Rencana Aksi Nasional (RAN) Konservasi Penyu Periode 2016-2020. Direktorat Jenderal Pengelolaan Laut, Kementerian Kelautan dan Perikanan.

Ko, B.C., Kim, H.H. and Nam, J.Y., 2015. Classification of potential water bodies using Landsat 8 OLI and a

combination of two boosted random forest classifiers. *Sensors*, 15(6): 13763-13777.

Marelsa, N.F. and Oktaviandra, Y. 2019. Analisis Karakteristik Gelombang Laut Menggunakan Software Windwave-12 (Studi Kasus: Kepulauan Mentawai). *OSEANA*, 44(2): 10-24.

Marpaung, S. and Harsanugraha, W.K. 2014. Analysis of Sea Surface Height Anomaly Characteristics Based on Satellite Altimetry Data (Case Study: Seas Surrounding Java Island). *International Journal of Remote Sensing and Earth Sciences*, 11(2): 37-142.

Maurer, A.S. and Johnson, M.W. 2017. Loggerhead Nesting In The Northern Gulf Of Mexico: Importance Of Beach Slope To Nest Site Selection In The Mississippi Barrier Islands. *Chelonian Conservation and Biology*, 16(2): 250-254.

Mbay, L.O.N. and Nurjaya, I.W. 2011. Arus Pantai Jawa pada Muson Barat Laut dan Tenggara di Barat Daya Sumatra. *Widyariset*, 17(2): 469-477.

Mukhtar, D. F. 2019. *Prediksi Dampak Kenaikan Muka Air Laut Akibat Perubahan Iklim Terhadap Habitat Peneluran Penyu Di Pantai Goa Cemara Kabupaten Bantul, Daerah Istimewa Yogyakarta*. Disertasi. Universitas Brawijaya.

Mustaqim, R. A., Sunarto, S., Syamsuddin, M. L., and Faizal, I. 2020. Abrasion Impact Towards Green Turtle Chelonia mydas (Linnaeus, 1758) Nesting Areas In Sindangkerta, Tasikmalaya Regency, West Java, Indonesia. *World Scientific News*, 147: 124-139.

Mutaqin, B. W., Kurniawan, I. A., Airawati, M. N., and Marfai, M. A. 2021. Kajian Perubahan Garis Pantai Di Sebagian Wilayah Pesisir Pandeglang, Banten, Periode Tahun 1990-2020. Jurnal Kelautan: *Indonesian Journal of Marine Science and Technology*, 14(3): 232-242.

Nasiti, I.P. and Sunarto, S. 2017. Perbandingan Karakteristik Geomorfik Habitat Peneluran Penyu Di Wilayah Pesisir Goa Cemara, Kabupaten Bantul dan Pangumbahan, Kabupaten Sukabumi. *Jurnal Bumi Indonesia*, 6(4).

National Oceanic and Atmospheric Administration (NOAA). 2023. Landsat Science. https:// landsat.gsfc.nasa.gov/ satellites/landsat-next. Diakses pada 12 Mei 2023 (10:22 WIB).

National Oceanic and Atmospheric Administration Fisheries (NOAA). 2022. Olive Ridley Turtle. https://www. fisheries.noaa.gov/ species/olive-ridley-turtle. Diakses pada 9 Mei 2023 (20:52 WIB).

Nuitja, I.N. and Uchida, I. 1983. Studies'in The Sea Turtles-Ii: The Nesting Site Characteristics of the Hawksbill and the Green Turtles. *Treubia*, 29(1): 63-79.

Nuitja, I.N.S. 1992. *Biologi Dan Ekologi Pelestarian Penyu Laut*. Penerbit IPB. Bogor.

Nuzula, F., Yuliadi, L.P.S. and Syamsudin, M.L. 2016. Variabilitas Temporal Eddy di Perairan Makassar–Laut Flores. *Jurnal Perikanan Kelautan*, 7(1).

Nybakken, J.W. and Bertness, M.P. 2005. *Marine Biology An Ecological Approach* 6thed. Person Education. San Francisco.

Pariwono, J.I. 1989. *Gaya Penggerak Pasang Surut Dalam Pasang Surut.* P3O -LIPI. Jakarta.

Pranowo, W.S., Tussadiah, A., Syamsuddin, M.L., Purba, N.P. and Riyantini, I. 2016. Karakteristik Dan Variabilitas Eddy Di Samudera Hindia Selatan Jawa. *Jurnal Segara*, 12(3): 159-165.

Purwanto, P., Tristanto, R., Handoyo, G., Trenggono, M. and Suryoputro, A.A.D. 2020. Analisis Peramalan dan Periode Ulang Gelombang di Perairan Bagian Timur Pulau Lirang, Maluku Barat Daya. *Indonesian Journal of Oceanography*, 2(1): 80-89.

Rifai, A., Rochaddi, B., Fadika, U., Marwoto, J. and Setiyono, H. 2020. Kajian Pengaruh Angin Musim Terhadap Sebaran Suhu Permukaan Laut (Studi Kasus: Perairan Pangandaran Jawa Barat). *Indonesian Journal of Oceanography*, 2(1): 98-104.

Rini, D.N. 2022. *Kajian Karakteristik Gelombang Pecah Di Pantai TPI Pulau Bunyu, Kabupaten Bulungan*. Skripsi. Universitas Borneo Tarakan. Tarakan

Rizqiyanto, F. A. 2022. *Studi Perubahan Garis Pantai Pulau Tabuhan Kecamatan Wongsorejo Kabupaten Banyuwangi Menggunakan Citra Google Earth*. Disertasi. UIN Sunan Ampel Surabaya.

Rofiah, A., Hartati, R. and Wibowo, E. 2012. Pengaruh naungan Sarang Terhadap Persentase Penetasan Telur Penyu Lekang (Lepidochelys olivacea) di Pantai Samas Bantul, Yogyakarta. *Journal Of Marine Research*, 1(2): 103-108.

Saputro, M., dan Nawawi, M. 2010. *Analisis Abrasi Pantai Semarang Bagian Barat (Analysis of The Western Part of Semarang Coastal Abration)*. Disertasi. Universitas Diponegoro.

Sari, Y.N., Wirasatriya, A., Kunarso, K., Rochaddi, B. and Handoyo, G. 2020. Variabilitas Arus Permukaan Di Perairan Samudra Hindia Selatan Jawa. *Indonesian Journal of Oceanography*, 2(1): 1-7.

Sears, F.W and Zemansky, M.W. 1982. *Fisika Untuk Universitas 1; Mekanika, Panas, Bunyi*. Penerbit Bina Cipta. Bandung.

Septiadi, R., Bengen, D.G. and Natih, N.M.N. 2018, July. Typology of Olive Ridley turtle (Lepidochelys olivacea, Linn 1958) nesting habitat in Kuta Beach, Serangan Beach and Saba Beach, Bali Province. IOP Conference Series: *Earth and Environmental Science*, 176(1): 012024.

Setiani, M. F. D. A. 2017. *Deteksi Perubahan Garis Pantai Menggunakan Digital Shoreline Analysis System (DSAS) di Pesisir Timur Kabupaten Probolinggo, Jawa Timur*. Disertasi. Universitas Brawijaya.

Sifuentes-Romero, I., Tezak, B.M., Milton, S.L. and Wyneken, J. 2018. Hydric Environmental Effects On Turtle Development And Sex Ratio. *Zoology*, 126: 89-97.

Sinulingga, H. A., Muskananfola, M. R., and Rudiyanti, S. 2018. Hubungan Tekstur Sedimen dan Bahan Organik Dengan Makrozoobentos Di Habitat Mangrove Pantai Tirang Semarang. *Management of Aquatic Resources Journal (MAQUARES)*, 6(3): 247-254.

Surinati, D. and Wijaya, J.H.M. 2017. Arus Selatan Jawa. *Oseana*, 42(3): 1-8.

Syaharani, L., and Triyatno, T. 2019. Analisis Perubahan Garis Pantai Kabupaten Padang Pariaman dan Kota Pariaman Tahun 1988-2018 Menggunakan Digital Shoreline Analysis System (DSAS). *Jurnal Buana*, 3(5): 1056-1067.

Triatmodjo, B. 1999. *Teknik Pantai*. Beta Offset. Yogyakarta.

Triyatno, T. 2014. Transportasi Sedimen Pantai Padang Sumatera Barat. *Jurnal Geografi*, 3(2): 77-84.

Tyas, D.W. and Dibyosaputro, S., 2012. Pengaruh Morfodinamika Pantai Glagah, Kabupaten Kulonprogo, Daerah Istimewa Yogyakarta Terhadap Keselamatan Pengunjung Pantai. *Jurnal Bumi Indonesia*, 1(3): 77008.

U.S. Geological Survey (USGS). 2023. Earth Exploler. https://earthexplorer.usgs.gov/. Diakses pada 29 Desember Mei 2022 (19:14 WIB).

Wahyuni, A., Fuadi, N., Zelviani, S., Ayu, D., Aminah, A., Azyurah, Z., and Nur, F. 2019. Pengukuran Strike Dan Dip Di Desa Padaelo'kecamatan Mallawa Kabupaten Maros Sulawesi Selatan. JFT: *Jurnal Fisika Dan Terapannya*, 6(1): 47-54.

Waluya, B. 2008. *Pengelolaan Lingkungan Hidup untuk Tk SMA*. Bandung: UPI.

Wisudo, HS. 2012. *Konservasi Sumber Daya Perairan*. Buku Materi Pokok LUHT4455. Universitas Terbuka. Tangerang Selatan.

Wyrtki, K. 1961. Physical Oceanography of the Southeast Asian Waters. Scripps Institution of Oceanography, The University of California, La Jolla.